Binding of herpes simplex virus-1 US11 to specific RNA sequences

Kevin F. Bryant[1,2], J. Colin Cox[3], Hongming Wang[1], James M. Hogle[1,2], Andrew D. Ellington[3] and Donald M. Coen[1,2,*]

[1]Department of Biological Chemistry and Molecular Pharmacology and [2]Committee on Virology, Harvard Medical School, 250 Longwood Avenue, Boston, MA 02115, USA and [3]Department of Chemistry and Biochemistry, University of Texas, Austin, TX, USA

ABSTRACT

Herpes simplex virus-1 US11 is a RNA-binding protein with a novel RNA-binding domain. US11 has been reported to exhibit sequence- and conformation-specific RNA-binding, but the sequences and conformations important for binding are not known. US11 has also been described as a double-stranded RNA (dsRNA)-binding protein. To investigate the US11–RNA interaction, we performed *in vitro* selection of RNA aptamers that bind US11 from a RNA library consisting of >10^{14} 80 base sequences which differ in a 30 base randomized region. US11 bound specifically to selected aptamers with an affinity of 70 nM. Analysis of 23 selected sequences revealed a strong consensus sequence. The US11 RNA-binding domain and ≤46 bases of selected RNA containing the consensus sequence were each sufficient for binding. US11 binding protected the consensus motif from hydroxyl radical cleavage. RNase digestions of a selected aptamer revealed regions of both single-stranded RNA and dsRNA. We observed that US11 bound two different dsRNAs in a sequence nonspecific manner, but with lower affinity than it bound selected aptamers. The results define a relatively short specific sequence that binds US11 with high affinity and indicate that dsRNA alone does not confer high-affinity binding.

INTRODUCTION

RNA-binding proteins play a role in many aspects of cellular biology, especially in the regulation of gene expression, where they are involved in virtually every stage (1). Because RNA-binding proteins play such an important role in regulating gene expression, and viruses often need to alter the gene expression profile of the host cell to produce an environment that is conducive to efficient viral replication, it is not surprising that many viruses encode RNA-binding proteins that may function to alter the expression patterns of viral and/or cellular genes.

One such RNA-binding protein, herpes simplex virus-1 (HSV-1) US11, is a relatively small (∼23 kDa), highly basic phosphoprotein (2) that is expressed late in infection but is present at early times post-infection as it enters the cell as a component of the virion (3). US11 is not necessary for viral replication in cell culture or in a mouse model (4) and its function in the HSV-1 lifecycle remains unclear. There have, however, been some reports regarding potential functions of the protein such as a role in axonal transport of the virion (5) and the regulation of gene expression (6–10).

The domain of US11 that is sufficient to bind RNA is located within the C-terminal half of the protein, and contains an amino acid sequence that consists almost entirely of a variable number (20–24, depending on strain) of R-X-P tripeptide repeats, where X is most commonly an acidic or uncharged polar amino acid (11). This RNA-binding domain (RBD) shows some homology to the Epstein–Barr virus SM protein (12), but it is not homologous to any other known proteins and thus the mechanism by which it recognizes and binds RNA may be novel.

US11 has been reported to bind a limited number of cellular and viral RNAs (2,3,10,13–16), but the functional relevance of these interactions has not yet been determined. In addition, although US11 has been reported to be a sequence- and conformation-specific RNA-binding protein (14,17), the sequences and/or conformations that confer binding of a RNA molecule to US11 have not been clearly elucidated.

The smallest natural RNA reported to be sufficient for US11 binding is a rather long sequence, 319 bases derived from the 5′ end of the *UL34* transcript (15). The dissociation constant (K_d) of the interaction between US11 and a RNA containing 319 bases of *UL34* sequence along with ∼50 bases of vector sequence is 100–130 nM *in vitro* (16), which is the highest affinity binding reported for a specific RNA–US11 interaction.

More recently, Khoo *et al.* (17) selected short RNA molecules (aptamers) that bound US11-RBD *in vitro* but these contained no consensus sequence (17). They also reported that the US11-RBD was able to bind double-stranded RNA (dsRNA) *in vitro* containing sequences distinct from their selected aptamers. From these and other data they concluded that US11 is a dsRNA-binding protein.

To gain more insight into how US11 binds RNA ligands, we used an automated procedure to select RNA aptamers that bind US11. We characterized the binding reaction, including quantification of the affinity of the US11–aptamer interaction. In addition, we have investigated the secondary structure of one of the selected aptamers and identified a shorter sequence within this aptamer that is sufficient to bind US11. We also compared the interaction of US11-RBD with the selected aptamers to its interaction with double-stranded aptamer RNA.

MATERIALS AND METHODS

Expression and purification of recombinant proteins

US11 sequences, encoding both full-length protein and the reported RBD, from HSV-1 strain KOS (GenBank accession no. AY832929) were PCR amplified (full-length US11 primers: US11N001 and US11C162; RBD primers: US11-RBD-R and US11-RBD-L; all primer sequences can be accessed as Supplementary Data, Table S1) and the resulting product contained engineered EcoRI and HindIII restriction sites at the 5′ and 3′ ends, respectively. The EcoRI/HindIII digested PCR product was cloned into EcoRI/HindIII digested pMAL-pp, which is a plasmid derived by A. Pearson from pMAL-c2X [New England Biolabs (NEB)] to contain a PreScission Protease site inserted into the XmnI restriction site, between sequences encoding maltose-binding protein (MBP) and its fusion partner (in this case, US11) (18). The resulting plasmids were named pMAL-pp-US11 and pMAL-pp-US11RBD. US11 sequences in these plasmids matched KOS genomic sequences. Expression of recombinant proteins from *E.coli* strain BL21(DE3)pLysS (Novagen) was induced with 0.3 mM isopropyl-β-D-thiogalactopyranoside (Fisher Biotech) and the cells were grown at 37°C for 4 h after induction. Cells were then pelleted and resuspended in buffer A (30 mM Tris–HCl, pH 7.5, 2 mM DTT, 0.5 mM EDTA and 5% glycerol) in addition to 1× Complete protease inhibitor cocktail (Roche) and 1 M NaCl. The resuspended pellet was frozen at −80°C. The cells were thawed slowly at 4°C and the cells were disrupted by sonication. Cellular debris was pelleted by centrifugation for 20 min at 30 000 *g* and the supernatant was applied to a column of amylose resin (NEB), equilibrated with the buffer A and 1 M NaCl. The amylose column was washed with three column bed volumes buffer A and 10 mM NaCl. Bound protein was eluted with this buffer containing 10 mM maltose. The eluate from the amylose column was applied to a 1 ml HiTrap Heparin HP column (Amersham Biosciences)

equilibrated with 20 ml buffer A and 10 mM NaCl. Bound protein was washed with 20 ml of this buffer and was then eluted in buffer A with a 10 mM–2 M gradient of NaCl. Fractions were monitored by SDS–PAGE and fractions containing US11 were pooled. Additional glycerol (to 25%) was added to the fractions containing purified MBP-US11 or MBP-US11-RBD and the protein samples were stored at −20°C. The concentration of the purified recombinant proteins was determined by amino acid analysis performed by the Molecular Biology Core Facility at the Dana Farber Cancer Institute. The purified protein was determined to be >90% active as assayed by the amount of RNA that a fixed amount of US11 bound when titrated to saturation with increasing concentrations of RNA. Purified recombinant MBP-UL42 was provided by John Randell.

In vitro selection of anti-US11 RNA aptamers

Automated selection experiments were carried out on a robotic workstation specifically adapted for the task as described previously (19,20). Briefly, the selection target, MBP-US11, was chemically conjugated to biotin (19) and was then immobilized on streptavidin-coated magnetic beads (Dynal, Lake Success, NY). A nucleic acid pool that contained a random sequence region that spanned 30 residues [N30; (21)] and that had a diversity of roughly 1.1×10^{14} unique sequences was incubated with the target-coated beads in the presence of selection binding buffer (50 mM Tris, pH 7.5, 200 mM NaCl, 5 mM $MgCl_2$ and 1 mM DTT). Nucleic acid binding species were partitioned from the randomized pool by vacuum filtration of the target-beads followed by four washes of 250 μl of the selection binding buffer (20). Bound species were eluted from the MBP–US11 complex and amplified by performing reverse transcription using AMV reverse transcriptase (AP Biotech), PCR using Display *Taq* (Promega) and *in vitro* transcribed using T7 RNA polymerase (Stratagene) into a new RNA pool for further rounds of selection and amplification as described previously (19,20). Overall, 12 rounds of automated selection were performed against this target under identical wash conditions for each round of selection. This procedure is shown using a schematic diagram in Figure 1. Upon completion of the 12th round of selection, reverse transcription and PCR, DNA products were cloned into pCR2.1 with Invitrogen's TA cloning kit according to the manufacturer's instructions. Selected clones were sequenced using a Dye Terminator Cycle Sequencing Kit (Beckman Coulter) on a CEQ 200XL capillary DNA sequencer (Beckman Coulter).

Synthesis of aptamer RNA

Full-length, 80 base, aptamer RNAs were *in vitro* transcribed from a PCR product containing a T7 promoter using the T7 MEGAshortscript kit (Ambion) according to the manufacturer's instructions. The primers (41.30 and 24.30) used to generate this PCR product were annealed to the constant sequences flanking the 30 bases of randomized sequence, and thus were the same for each aptamer clone. 'Cut' aptamer RNA was generated essentially in the same manner, with the exception that the PCR product used as a template in the *in vitro* transcription reaction was digested with SfcI. The SfcI digested *in vitro* transcription template was gel purified to ensure that undigested templates were not present in the
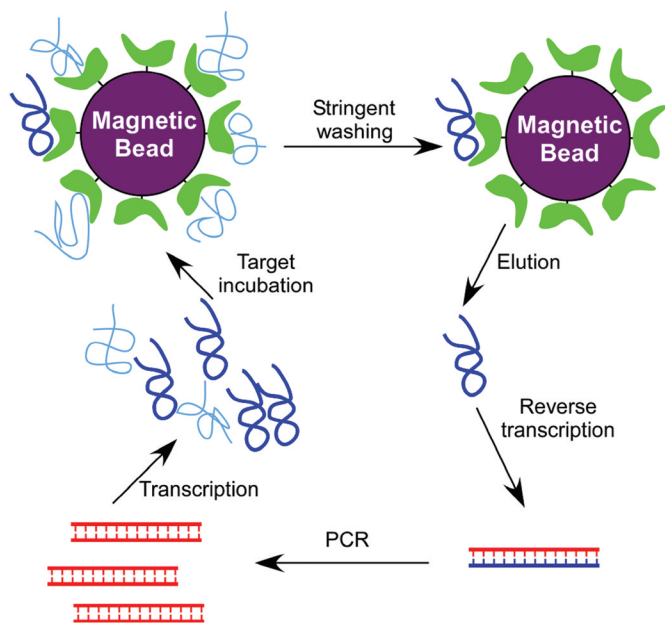
Figure 1. Simplified scheme for *in vitro* RNA selection. A random RNA pool (RNA shown as blue squiggles) is incubated with the selection target, MBP-US11 (shown as green crescents), immobilized on magnetic beads (shown as purple circles). The bead-bound complexes are washed to remove low-affinity nucleic acid binding species (thin blue squiggles). Next, tightly bound RNA molecules (thick blue squiggles) are eluted from the target and reversed transcribed, PCR amplified, and *in vitro* transcribed in order to regenerate the RNA pool. The delimited pool is then incubated with a new aliquot of the immobilized target, and the selection cycle begins again.

transcription reaction. The SfcI digestion removed 15 bp from the 3′ end of the PCR product and the resulting transcribed RNA is 65 bases in length. The template for the 'short' aptamer RNA was generated by amplifying a PCR product with an upstream primer that annealed to the sequence just upstream of the 30 base randomized sequence (C17 short). This PCR product is missing 19 bases from the 5′ end compared with the full-length template and the transcribed RNA is 61 bases long. To generate the template for the 'short cut' aptamer RNA, we digested the 'short' template with SfcI and gel purified the digested product. *In vitro* transcribed RNA was labeled internally by including [α-^{32}P]UTP [1.6 μM final concentration and 800 Ci/mmol (NEN)] in the *in vitro* transcription reaction, in addition to the unlabeled nucleotides (ATP, CTP and GTP are 7.5 mM final concentration, UTP is 5.6 mM). *In vitro* transcribed RNA was purified by phenol/chloroform extraction followed by ethanol precipitation in the presence of either 0.3 M sodium acetate or 0.75 M ammonium acetate after stopping the reaction by digesting the DNA template with DNaseI. The pellet was washed twice with 70% ethanol and resuspended in water. The RNA concentration was determined by analyzing the amount of trichloroacetic acid insoluble counts present as described previously (22).

Electrophoretic mobility shift assays (EMSAs)

All EMSAs were performed essentially as described previously (23). Briefly, 5 nM internally labeled aptamer RNA was incubated with various concentrations of protein in the presence of 1× binding buffer (50 mM Tris, pH 8, 100 mM

NaCl and 14.4 mM 2-mercaptoethanol), 30 μg yeast tRNA (Ambion), MTPBS and 20 U SUPERase•In (Ambion). Binding was allowed to reach equilibrium by incubating samples for 30 min at room temperature unless otherwise noted. An aliquot of 1 μl loading buffer (0.025% bromophenol blue, 0.5× TBE and 10% glycerol) was added to each reaction and the entire reaction was resolved on a 5% non-denaturing polyacrylamide gel. RNA was visualized using dried gels to expose a phosphor storage screen and the data were analyzed using the Quantity One program (Bio-Rad).

Fe-EDTA hydroxyl radical footprinting

Aptamer RNA was *in vitro* transcribed as described above with the exception that [α-^{32}P]ATP was not included and 7.5 mM of all NTPs were used. This RNA was purified by phenol/chloroform extraction followed by ethanol precipitation in the presence of 0.75 M ammonium acetate. The RNA pellet was washed with 70% ethanol and resuspended in water. This RNA was dephosphorylated by calf intestinal alkaline phosphatase and phosphorylated with polynucleotide kinase using [γ-^{32}P]ATP [167 μCi/μl, >7000 Ci/mmol (ICN)] using the KinaseMax kit (Ambion). Labeled RNA was resolved on a 12% denaturing polyacrylamide gel and the full-length product was visualized by autoradiography, and the corresponding gel slice was excised and crushed with a pipette tip. RNA was eluted from the crushed gel overnight in 300 μl in crush and soak buffer (500 nM NH$_4$OAc, 10 mM Mg(OAc)$_2$, 1 mM EDTA and 0.1% SDS) at 4°C, followed by a second elution step with 100 μl crush and soak buffer for 1 h at 37°C. Eluted RNA was phenol/chloroform extracted, ethanol precipitated and washed with 70% ethanol and the pellet was resuspended in RNA renaturation buffer (10 mM NaH$_2$PO$_4$, 50 mM NaCl, 3 mM MgCl$_2$ and 0.1 mM EDTA). RNA was denatured by heating to 80°C for 5 min and renatured by slowly cooling the sample to 25°C at a rate of 0.033°C/s. Binding reactions with MBP-US11-RBD were performed as described above with the exception that 1.5 μg yeast tRNA was added, rather than 30 μg. After the binding reaction was allowed to reach equilibrium, 1 μl each of 25 mM ammonium iron (II) sulfate hexahydrate, 50 mM EDTA, 100 mM ascorbic acid and 3% hydrogen peroxide were added to the reaction. Samples were incubated for 1 min at room temperature, vortexed and incubated for an additional minute at room temperature. The reaction was stopped by the addition of 100 mM thiourea. Following the hydroxyl radical cleavage reaction, the samples were phenol/chloroform extracted and ethanol precipitated in the presence of GlycoBlue (Ambion). Precipitated RNA was washed with 70% ethanol and resuspended in loading buffer II (Ambion). RNase T1 digestions and alkaline hydrolysis reactions were performed as directed by the manufacturer. Samples were resolved on a 12% sequencing gel (SequaGel; National Diagnostics) at a constant power of 40 W. The gel was dried and used to expose a Bio-Rad phosphor storage screen.

RNase digestion

Aptamer RNA was *in vitro* transcribed, end-labeled, purified, denatured and renatured in the same manner as the RNA prepared for Fe-EDTA footprinting. RNase digestions, as well as alkaline hydrolysis of the RNA were carried out

essentially as directed by the manufacturer (biochemistry grade RNase A, T1 and V1; Ambion). We used 10 and 1 ng RNase A, 0.1 and 0.01 U RNase T1 and 0.001 and 0.0001 U RNase V1 per reaction, each in a separate reaction. For alkaline hydrolysis, samples were incubated at 100°C for 2 and 5 min in alkaline hydrolysis buffer (Ambion). Following RNase digestion, reactions were stopped by ethanol precipitation of the RNA. The precipitated RNA was washed with 70% ethanol and was resuspended in loading buffer II (Ambion). Samples were resolved on a 12% sequencing gel (SequaGel; National Diagnostics) at a constant power of 40 W. The gel was dried and used to expose a Bio-Rad phosphor storage screen.

Generation of antisense and double-stranded aptamer RNA

The template used to *in vitro* transcribe RNA antisense to the selected aptamers was created by PCR using a set of primers that contain the T7 promoter on the opposite primer than that used to generate the templates for the sense strand aptamer RNA [41.30 (−T7) and 24.30 (+T7)]. Antisense RNA was *in vitro* transcribed, purified and quantified in the same manner as the sense strand aptamer RNA. dsRNA was generated by annealing sense and antisense strands as described previously (17). Unhybridized RNA was digested with 1000 U RNase T1 (cloned grade; Ambion) and 2 ng RNase A (biochemistry grade; Ambion) at room temperature. Following digestion, samples were resolved on a 5% non-denaturing polyacrylamide gel. The portion of the gel containing dsRNA was visualized by autoradiography, excised, eluted and purified as described above, with the exception that the RNA was resuspended in water. The double-stranded nature of the RNA was confirmed by its resistance to the single-strand-specific RNases A and T1 and sensitivity to the double-strand-specific RNase V1 (data not shown).

Determination of K_d values

The equation used to determine the K_d values in this report was derived from the following two equations: $r = (\bar{C}_S - C_S)/\bar{C}_A$ and $r = pC_S/(K_d + C_S)$ where r is a binding function defined as the molar ratio of the amount of bound ligand to the total amount of acceptor, p is the number of independent and equivalent binding sites on the acceptor (which we observed to be 1 for the selected aptamer acceptor and to be 3 for the double-stranded aptamer RNA acceptor), $\bar{C}_S$ is the total ligand concentration (which in this case is total protein concentration), C_S is the free ligand concentration (which in this case is unbound protein concentration), $\bar{C}_A$ is the total acceptor concentration (which in this case is total RNA concentration) (24). The two equations were set equal to each other to give the following equation: $(\bar{C}_S - C_S)/\bar{C}_A = pC_S/(K_d + C_S)$. Rearranging the terms in this equation to solve for K_d gives $K_d = pC_S\bar{C}_A/(\bar{C}_S - C_S) - \bar{C}_S$, which is the equation we used to calculate the K_d values in this report. K_ds were calculated using C_S = total protein since unbound protein was in great excess over bound protein. For the $(\bar{C}_S - C_S)$ term, which is the concentration of the bound protein–RNA complex, we used the concentration of bound RNA since this value could be directly measured. The K_ds were determined using a RNA concentration of 5 nM and a range of protein concentrations. K_ds are presented as an average of the values, measured in triplicate and obtained at each protein concentration.

RESULTS

In vitro selection of RNA aptamers that bind US11

We performed 12 rounds of automated selection for aptamers that bound MBP-US11. A total of 23 selected aptamers were cloned and sequenced, and from this pool there emerged a consensus (UUCGCAAUYCUGCAYUG, where Y is a pyrimidine base) within the selected sequences (Figure 2).

Figure 2. Selected anti-US11 aptamers. Sequences cloned from the random sequence pool after 12 rounds of selection and amplification are shown. The constant priming region is shaded in light gray; the random region is in black text and sequences with high similarity in the random region are highlighted in red text. The consensus sequence is shown at the bottom of the figure (Y = pyrimidine, C or U).

To investigate the specificity of the interaction of US11 with the selected aptamer RNA species, we performed EMSAs with purified recombinant MBP-US11 and *in vitro* transcribed aptamer RNA. This permitted us to assess whether the aptamers exist as one or more stable conformers and whether they contain one or more US11-binding sites. We analyzed four of the selected aptamers, clone 13 (C13), C16, C17 and C22, that differed from one another both inside and outside of the 17 nt consensus region (Figure 2). Figure 3A shows that aptamer C17 migrated as a single band on a native polyacrylamide gel in the absence of US11, suggesting that it exists as a single major conformer. With increasing concentrations of US11, a single band of lower mobility appeared, indicating that there is one specific US11-binding site present in this selected aptamer (Figure 3A). Similar data were obtained for each of the three other aptamers tested (data not shown).

To determine whether the RBD of US11 was sufficient for the observed binding, we expressed and purified this domain of US11 fused to MBP. This recombinant protein bound to the selected aptamer C17 (Figure 3B).

The aptamers were selected to bind US11 that was expressed and purified as an MBP fusion protein. To show that the binding was specific to the US11 moiety of the fusion protein, we performed EMSAs with MBP fused to another nucleic acid binding protein, UL42, which is the processivity factor for the HSV-1 DNA polymerase and can bind DNA with nanomolar affinity (25). MBP-UL42 did not bind the selected aptamer RNA detectably (Figure 3C), indicating that the interaction is specific to the US11 moiety.

To assess whether the US11–aptamer interactions were specific for the selected aptamers, we performed EMSAs with an aptamer that was not selected to bind US11. US11 did not detectably bind an aptamer that was selected to bind hen egg white lysozyme (lyso, sequence in Figure 4) (19), even at the highest concentrations of protein assayed (Figure 3D). To provide further evidence for the specificity of the interaction of US11 with the selected aptamers we also performed competition experiments in which unlabeled selected aptamers competed the binding of US11 from labeled selected aptamer RNA, but unlabeled lyso aptamer RNA did not compete binding (data not shown).

Mapping the US11-binding site on a selected aptamer

Since the US11–RNA EMSAs indicated that there is one binding site for US11 on the selected aptamers, we attempted to define a smaller RNA sequence that is sufficient to confer US11 binding. We made 5′ and/or 3′ truncations of the C17 aptamer RNA (Figure 4) and assayed the ability of these truncated RNAs to bind US11 by performing EMSAs. Deleting either the 5′ (short) or the 3′ (cut) end of aptamer C17 RNA resulted in RNA species that were still sufficient to bind US11 (Figure 5A and B). This indicates that although the constant flanking sequence at the ends of the RNA may contribute to the ability of RNA to bind US11, they are not necessary for US11 binding.

US11 also bound to a RNA species lacking both the 5′ and 3′ sequences (short-cut), but only ∼25% of this RNA was capable of binding *in vitro* at room temperature (data not shown). Much more RNA bound US11 when the EMSAs were
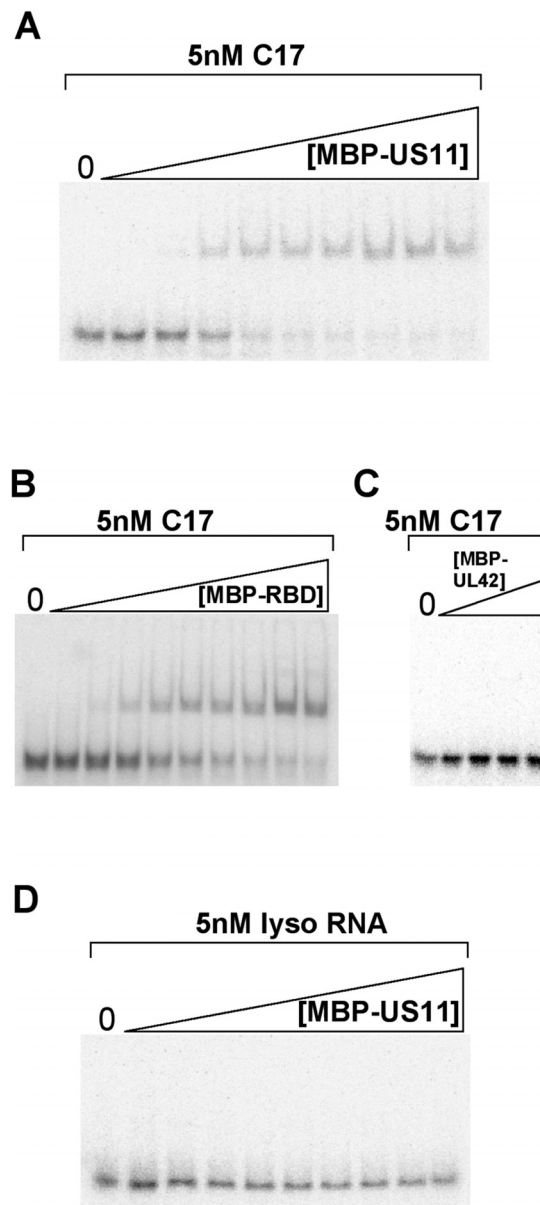

Figure 3. Binding of US11 to the selected aptamers is specific. (**A**) RNA EMSA was performed by incubating an internally labeled representative selected RNA aptamer, C17, either without protein (0), or with increasing concentrations of MBP-US11 (11.5, 23, 46, 92, 122, 183, 367, 550 and 1100 nM final concentrations). Bound complexes were resolved from free RNA by electrophoresis in 5% native polyacrylamide gels. (**B**) C17 RNA incubated with either no protein (0), or increasing concentrations of the RNA-binding domain of US11 fused to MBP (9.375, 18.75, 37.5, 76, 150, 300, 600, 1200 and 2400 nM final concentrations). (**C**) C17 RNA incubated with either no protein (0), or a protein that it was not selected to bind, MBP-UL42 (87.5, 185, 350 and 700 nM final concentrations). (**D**) RNA EMSA performed as in (A), with the exception that a RNA aptamer selected for binding to hen egg white lysozyme (lyso) was incubated with MBP-US11. All gels were dried and used to expose phosphor storage screens. Screens were then scanned by a Bio-Rad phosphorimager.

performed at 4°C (Figure 5C), most probably owing to a greater proportion of the RNA folding into a conformation that was competent to confer US11 binding. US11 bound full-length aptamers under these conditions with the same affinity as the case when the assay was performed at room temperature

RNA Species	RNA
	Consensus
C17	GGGAAUGGAUCCACAUCUACGAA**UUCGCAAUCCUGUAUUG**AACUUCUCACUAAAACUUCACUGCAGACUUGACGAAGCUU
short	GGAA**UUCGCAAUCCUGUAUUG**AACUUCUCACUAAAACUUCACUGCAGACUUGACGAAGCUU
cut	GGGAAUGGAUCCACAUCUACGAA**UUCGCAAUCCUGUAUUG**AACUUCUCACUAAAACUUCACUGC
short-cut	GGAA**UUCGCAAUCCUGUAUUG**AACUUCUCACUAAAACUUCACUGC
lyso	GGGAAUGGAUCCACAUCUACGAAUUCAUCAGGGCUAAAGAGUGCAGAGUUACUUAGUUCACUGCAGACUUGACGAAGCUU

Figure 4. Sequences of truncated aptamers. The sequences of aptamer C17, shorter versions of C17, and the aptamer selected to bind hen egg white lysozyme (lyso) used in the assays mapping the binding site on this aptamer are listed. Constant flanking sequences are listed in gray, the selected sequence is listed in black and the consensus sequence is in boldface.
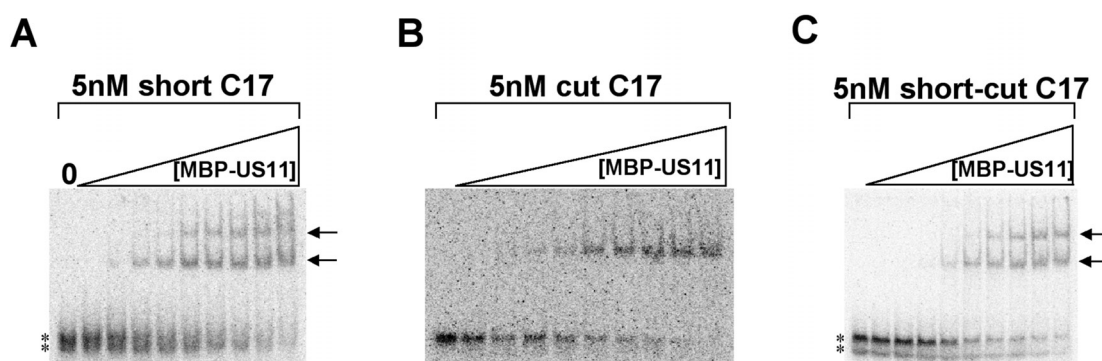

Figure 5. Mapping of US11-binding site on a selected aptamer. Internally labeled (**A**) short C17 RNA, (**B**) cut C17 RNA, or (**C**) short-cut C17 RNA incubated with either no protein (0), or increasing concentrations of MBP-US11 as described in the legend to Figure 1. Some RNAs existed as more than one conformation when not bound to protein [*: (A and C)], which may result in the additional shifted bands that appear at the high protein concentrations (arrows).

(data not shown). However, a shorter RNA oligonucleotide consisting of 21 bases, including the selected consensus sequence, did not bind US11 (data not shown). We conclude from these experiments that the binding site for US11 is contained within a 46 base segment of one of the selected aptamer RNAs, which consists mainly of the selected sequence and contains the consensus motif.

In the cases of short and short-cut RNAs, the free probe migrated as more than one band on a native polyacrylamide gel (Figure 5A and C). These RNAs migrated as one band on a denaturing gel (data not shown), which suggests that the multiple bands were structural conformers. In the presence of US11 there was also more than one shifted band on native gels (Figure 5A and C), suggesting that these truncated RNAs may fold into more than one detectable RNA conformer that can bind US11.

Fe-EDTA hydroxyl radical footprinting of US11-RBD

In an effort to map the US11-binding site on a selected aptamer more finely, we performed an Fe-EDTA hydroxyl radical footprinting assay. In this assay, US11-RBD protected a portion at the 5′ end of the selected sequence of aptamer C17, bases 26–43 (Figure 6). Increasing concentrations of US11-RBD led to decreasing levels of hydroxyl radical cleavage in this region and although the protection was not complete, it was reproducible. The region of RNA that was protected is present in the 46 base RNA that is sufficient to bind US11. In addition, the protected sequence corresponds almost exactly to the selected consensus motif, which is located in bases 24–40.

Binding of US11-RBD to aptamer C17 also resulted in sites more frequently cleaved by hydroxyl radical cleavage outside of the region that was protected, especially in the area 5′ to the protected segment (Figure 6). These data suggest that US11 may affect the higher order structure of RNAs that it binds, at least at close proximity to its binding site.

RNase structure mapping of selected aptamers

It has been reported that US11 binds RNA by a mechanism that is dependent on substrate RNA being in a specific conformation, possibly double-stranded in nature (14,17). In an effort to elucidate the RNA conformation of the sequences that bind US11, we attempted to determine the secondary structure of one of the selected aptamers, C17. We assayed the sensitivity and resistance to single-strand-specific RNases A and T1 and double-strand-specific RNase V1. The RNase digestion pattern indicated that this aptamer contains regions of both single-stranded and double-stranded nature throughout its length (Figure 7). In particular, there are multiple bases that are digested by the single-strand-specific RNases A (bases 28 and 36) and T1 (bases 27, 35 and 40) in the region of C17 that US11 protects from hydroxyl radical cleavage. There are also

bases in this region that were digested by the double-strand-specific RNase V1 (bases 25, 26, 34, 43–46, 48 and 51). These data indicate that US11 is able to recognize and bind a RNA that is not simply double-stranded.
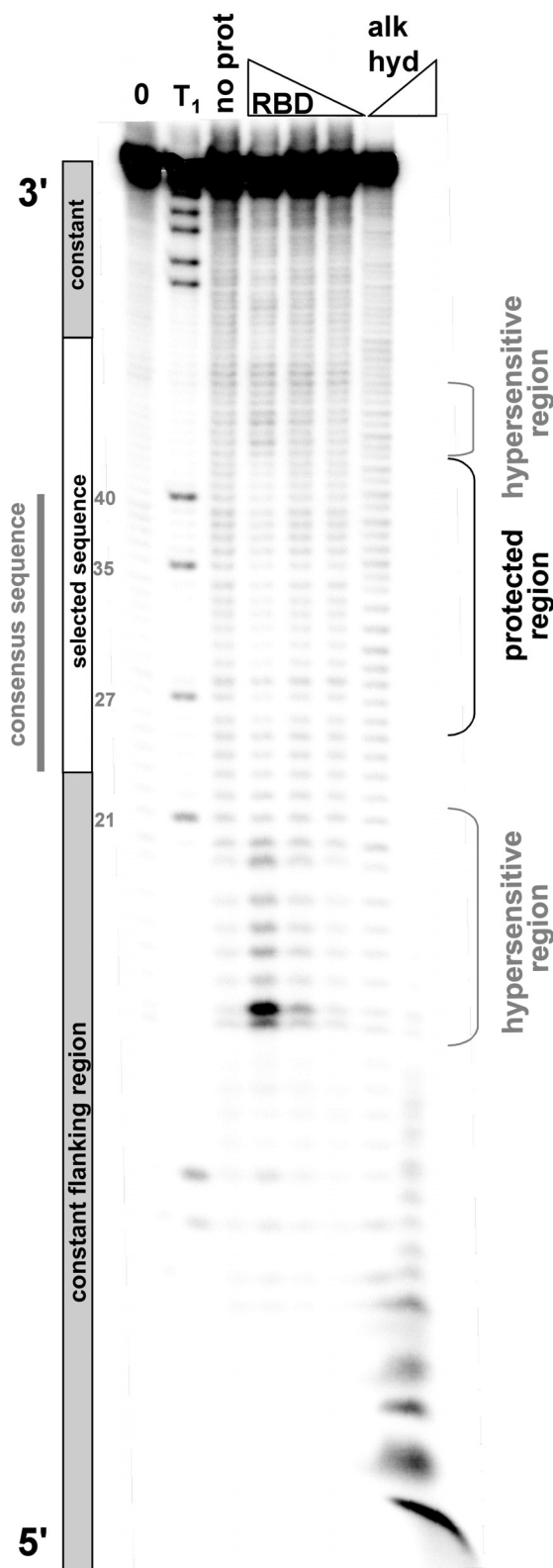
US11 binds double-stranded aptamer RNA, but non-specifically

To further investigate the ability of US11 to bind dsRNA, we made aptamer RNA double-stranded by hybridizing it to its complementary strand and determined how this affected US11 binding. In these experiments we examined two different aptamers, C17, which binds US11 and its RBD and the lyso aptamer, which did not show any detectable binding to US11 or its RBD. We performed the dsRNA-binding assays with the RBD of US11 since this was the domain that was used by Khoo *et al.* (17) to originally characterize the dsRNA-binding activity of US11. We first examined whether US11-RBD bound RNAs antisense (α) to either C17 or lyso to determine whether these sequences could contribute to any observed binding of US11-RBD to dsRNA. US11-RBD did not detectably bind either of the single-stranded antisense aptamer RNAs (Figure 8A and B). Since both the selected C17 sense and non-selected αC17 antisense aptamer RNAs contain the ability to form the same intramolecular double-stranded regions, yet only the selected C17 sequence can bind US11-RBD, the double-stranded nature of the aptamers is not alone sufficient to confer US11 binding. US11–RBD bound both double-stranded C17 and lyso aptamer species (Figure 8C and D). The observed binding of US11-RBD to the dsRNA differed qualitatively from binding to the single-stranded C17 aptamer, as indicated by the multiple shifted bands that appear as the concentration of US11-RBD increases (Figure 8C and D). This pattern of shifted bands is consistent with non-specific dsRNA binding by US11. At highest concentrations of US11-RBD, the probe primarily migrated as the band with slowest mobility. Since there are three major bands that appear with increasing US11-RBD concentration, these data suggest that the dsRNA aptamers can bind three molecules of US11-RBD, most probably without sequence specificity.

The US11-RBD binds selected aptamers with higher affinity than it non-specifically binds dsRNA

To further characterize the RNA-binding properties of US11, we determined the affinity of the interaction of US11 with a subset of the selected aptamers as outlined in Materials and Methods. Aptamer C17 bound US11 with a K_d of ~70 nM (example of data in Figure 3A).

Since US11-RBD seemed to bind selected aptamers differently from dsRNA, based on the different patterns of shifted bands, we next wanted to compare the affinity of US11-RBD for the selected aptamers to that for the dsRNA. The affinity for the interaction between US11-RBD and the selected aptamers was ~6-fold higher than the affinity of US11-RBD

Figure 6. Fe-EDTA hydroxyl radical footprinting of the MBP-US11-RBD–C17 RNA interaction. End-labeled C17 RNA was incubated with Fe-EDTA hydroxyl radical solution, as described in Materials and Methods, either in the presence of US11 buffer (no prot) or in the presence of decreasing concentrations of MBP-US11-RBD (19, 3.8 and 0.76 μM final concentrations). These RNAs were also digested with RNase T1 under denaturing conditions (T1) and cleaved by alkaline hydrolysis (alk hyd) to help determine where in the RNA the footprints were located. Untreated RNA was also run (0). A schematic of the aptamer RNA is diagrammed to the left of the gel, along with the consensus motif, and the regions of the RNA that are protected from or hypersensitive to hydroxyl radical cleavage are diagrammed to the right of the gel. Bases sensitive to digestion by RNase T1 are numbered to the right of the aptamer schematic diagram.
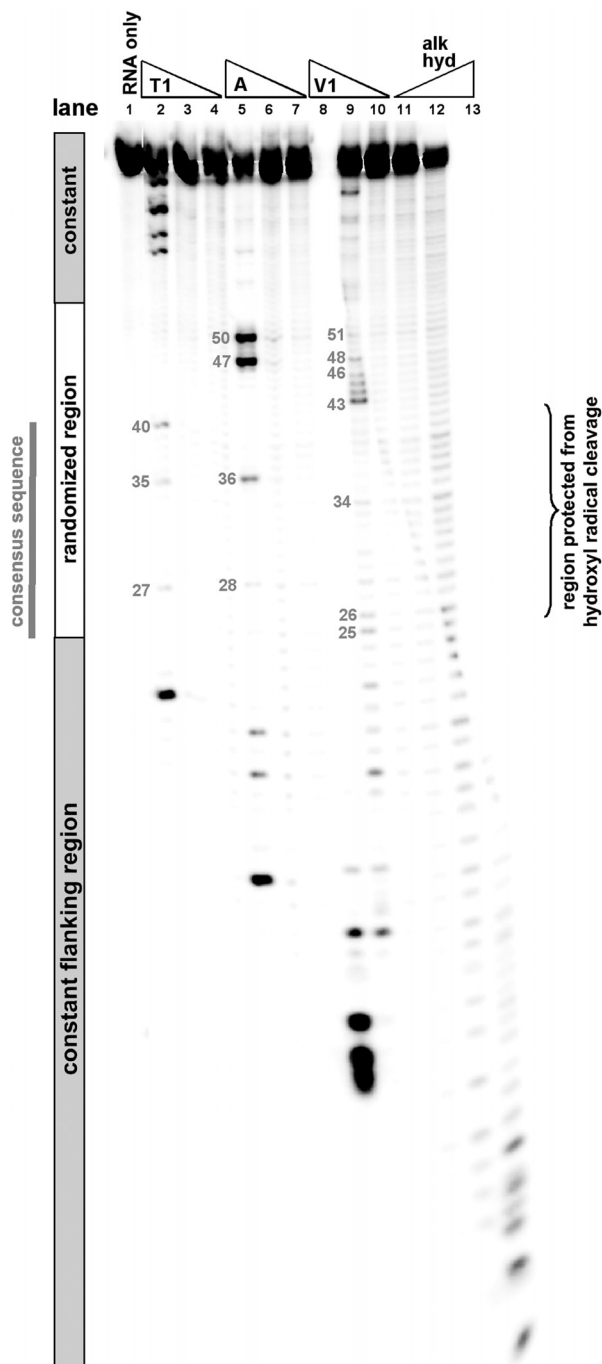
Figure 7. RNase structure mapping of a selected aptamer. End labeled C17 RNA was digested with RNases A, T1 and V1, as described in Materials and Methods, to determine regions of the RNA that had single-stranded or double-stranded nature. C17 RNA was also run untreated (lane 1) and was cleaved by alkaline hydrolysis (lanes 11–13). A schematic of the aptamer RNA is diagrammed to the left of the gel, along with the consensus motif. Bases sensitive to digestion by the various RNases are numbered. The region of RNA protected from Fe-EDTA hydroxyl radical footprinting is shown on the right of the gel. A diagonal line in lanes 9–13 is a result of a crease in the gel created as the gel was dried.

for dsRNA. The K_d for the US11-RBD–C17 interaction was 220 nM and the K_d for the interaction between US11-RBD and either species of dsRNA was ~1200–1400 nM (Table 1). Therefore, in addition to US11-RBD binding to dsRNA in a

seemingly non-specific manner, this interaction has a lower affinity than its specific interaction with the selected aptamers.

DISCUSSION

US11 binds tightly and specifically to the selected aptamers

After we initiated our study, Khoo *et al.* (17) reported selection of aptamers that bind US11-RBD. However, their study did not measure the affinity of binding to any of the aptamers. Additionally, the size and location of the US11-binding site within their selected aptamers were not reported and there did not appear to be an obvious sequence consensus motif selected. In their study, the selected aptamers seem to adopt multiple conformations that differed in their ability to bind US11 but the structures of the conformers that were competent to confer US11 binding were not investigated. Since this previous study left some questions regarding RNA binding by US11 unanswered, we continued our studies in an attempt to better define the RNA-binding properties of US11.

The RNA molecules that we selected *in vitro* have the ability to bind US11 with high affinity; the K_d for the US11–C17 aptamer RNA interaction is ~70 nM. This is the highest affinity yet reported for a specific US11–RNA interaction. Unlike the aptamers selected by Khoo *et al.* (17), we observed one free probe band and one specific shifted band upon US11 binding for our selected aptamers, indicative of one major conformer in each state. We interpret these data to mean that there is one detectable binding site for US11 on the selected aptamers, and that the binding is specific. This binding seems to be predominantly mediated by the RBD of US11.

Upon analysis of the sequences of the aptamers that bind US11, there emerged a strong consensus motif in the 5′ half of the selected sequence (Figure 2, UUCGCAAUYCUGCA-YUG, where Y indicates a pyrimidine base). However, neither this consensus nor any of the selected aptamer sequences seem to be present in the HSV-1 genome. It is possible that we did not identify sequences previously known to bind US11, including the sequences selected *in vitro* by Khoo *et al.* (17), because these interactions may have a lower affinity, and thus would not be selected by our protocol. Alternatively, the sequences known to bind US11 may fold into structures that mimic the structure of our selected aptamers and these structures may be more important for US11 binding than the primary sequence of the RNA.

US11 binds to a specific aptamer segment

The binding site for US11 in one of these selected aptamers, C17, was 46 bases or less in length, mainly consisting of the selected RNA sequence. This is the shortest sequence reported to be sufficient for binding US11. The consensus sequence lies within the short-cut 46 base aptamer and experiments assaying hydroxyl radical footprinting of US11-RBD binding revealed that this region is protected. These data suggest that the consensus motif is a determinant that forms at least part of the US11-binding site.
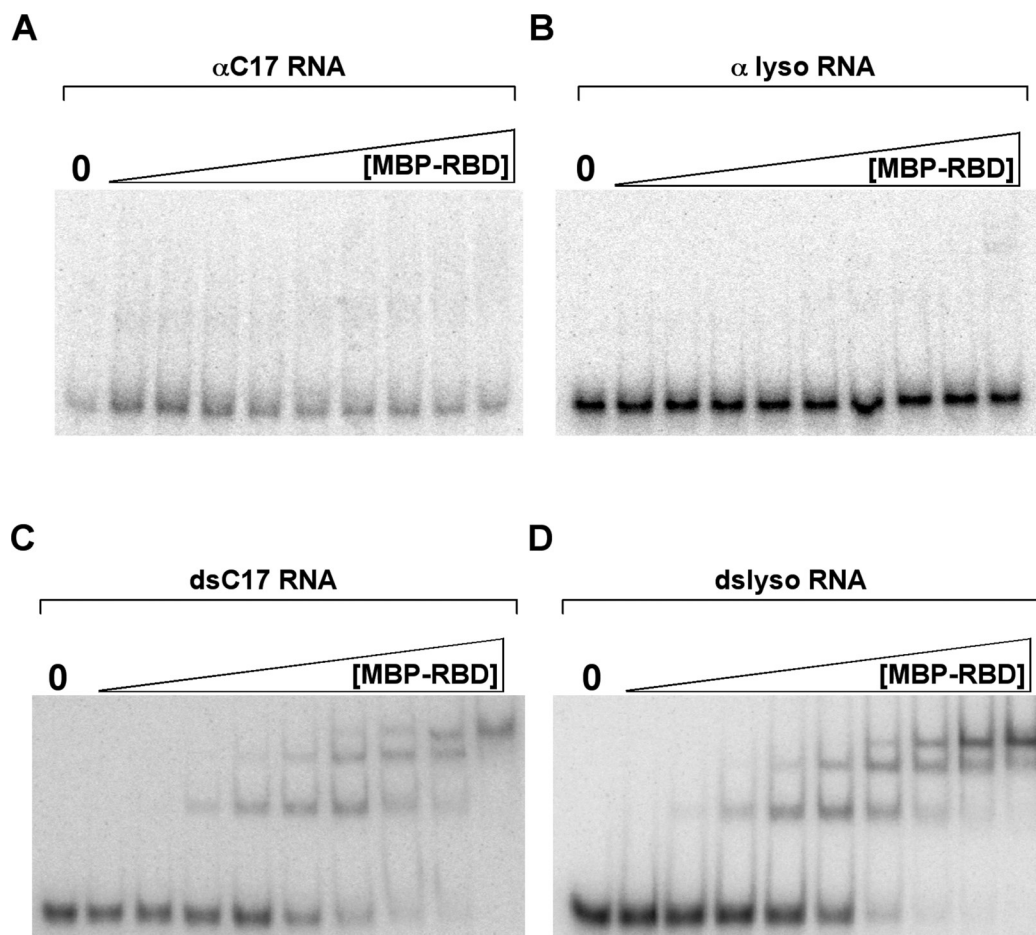
Figure 8. Non-specific binding of MBP-US11-RBD to dsRNA. (**A**) Internally labeled antisense aptamer C17 was incubated with either no protein (0), or increasing concentrations of MBP-US11-RBD (9.375, 18.75, 37.5, 75, 150, 300, 600, 1200 or 2400 nM final concentrations). (**B**) Antisense lyso aptamer, (**C**) double-stranded C17 RNA and (**D**) double-stranded lyso RNA was incubated with or without protein as in (A).

Table 1. Dissociation constants (K_ds) for binding of RNAs by US11-RBD

RNA	K_d (nM)
C17	220 ± 60[a]
Lyso	n.d.[b]
dsC17	1400 ± 170
dsLyso	1200 ± 200

[a]Values reported ± SD.
[b]No binding detected.

Data generated from RNase structure mapping indicate that selected aptamer C17 forms a structure that contains both single-stranded RNA and dsRNA sequences. The region of the RNA that is protected from hydroxyl radical cleavage also contains regions of both single-stranded RNA and dsRNA. It has been previously reported that US11 can bind specific RNA structures (14,17), in particular dsRNA (10). However, neither the structures of the viral or cellular US11 ligands that have been reported nor the aptamers selected by Khoo *et al.* (17) have been investigated. Our data indicate that a RNA, which is not completely double-stranded, is able to bind US11 with high affinity *in vitro*, and provide the first experimental evidence that there are structures other than simple dsRNA recognized by US11.

US11 binds dsRNA differently than it binds selected aptamers

US11 has recently been reported to bind dsRNA *in vitro*, and accordingly, it has been termed a dsRNA-binding protein (17). Although this study showed that US11 can bind dsRNA, we examined the US11–dsRNA interaction in greater detail to determine whether there were any discernible differences between this mode of binding and the specific binding of US11 to the selected aptamers. Our data indicate that although US11 can bind dsRNA, the binding appears to be non-specific and the interaction has a lower affinity than the specific binding to selected aptamers. In the case of the lyso aptamer, neither the sense nor the antisense RNA can bind US11-RBD, but when these two strands are annealed, US11-RBD can bind to the resulting dsRNA. This binding exhibits an affinity and pattern of shifted bands as the binding similar to dsC17 RNA, which contains a sequence that US11-RBD specifically binds. This indicates that, in this case, the double-stranded nature of the RNA was the major determinant to confer US11 binding, rather than the sequence. To our knowledge, there has never been a report where US11 did not bind dsRNA, provided the dsRNA was of sufficient length. Given this, it is interesting that we did not select any aptamers that are

predicted to be highly double-stranded. This could be due to the lower affinity binding of US11 to these RNAs. It is also possible that our selection protocol may have preferentially reverse transcribed or PCR-amplified aptamers without extensive double-stranded nature, which might exclude some US11 ligands such as those that are double-stranded.

Khoo *et al*. (17) reported that His-tagged full-length US11 bound an 81 bp dsRNA with an apparent K_d of 12.6 nM (17). Our data raise the possibility that this value is an overestimate of the affinity as the filter binding assay used would not account for the multiple binding sites for US11 on the dsRNA. We also speculate that the positively charged His-tag might have contributed to binding.

Possible roles for US11 RNA binding during HSV-1 infection

US11 has been shown to bind dsRNA (17) and this binding may alter gene expression in infected cells. US11 plays a role in the global stimulation of translation late in infection (9), possibly through its interaction with dsRNA and/or other proteins that can bind dsRNA, such as PKR. However, if RNA molecules exist in infected cells that have sequences and/or structures that are similar to the selected aptamers, which US11 binds specifically with high affinity, it is possible that US11 would preferentially bind those RNA species rather than dsRNA, which US11 binds non-specifically with lower affinity. Such specific binding might also play a role in the viral lifecycle.

Examples of specific regulation of gene expression by US11 have previously been reported for the cases of viral genes *UL13* and *UL34* (10,15). In these reports, US11 has been reported to specifically bind the transcripts encoded by these genes, possibly by a mechanism similar to the specific binding of US11 to our selected aptamers. Our results raise the intriguing possibility that specific binding of RNAs by US11 could be required for the regulation of gene expression. Such binding could recruit *trans*-acting factors involved in the stimulation or inhibition of gene expression, impede the translational machinery, or alter RNA stability or the subcellular localization of bound transcripts. Since US11, when bound to selected aptamers, generates sites that are hypersensitive to hydroxyl radical cleavage, in addition to sites that are protected, it is possible that US11 may alter the higher order structure of RNA that it binds during infection. This could potentially alter the expression of bound transcripts by changing the profile of RNA-binding proteins able to bind these mRNAs and in turn also possibly change the subcellular localization, stability, or translational efficiency of these transcripts, all of which could alter their expression.

Since US11 has both specific and non-specific RNA binding activities *in vitro*, it is possible that US11 may also bind RNA via both mechanisms in infected cells and thus have both specific and non-specific activities in the regulation of gene expression during HSV-1 infection.

SUPPLEMENTARY DATA

Supplementary Data are available at NAR Online.

REFERENCES

1. Sandberg,K. and Mulroney,S.E. (2002) *RNA-Binding Proteins: New Concepts In Gene Regulation.* Kluwer Academic, Boston, MA.
2. Diaz,J.J., Simonin,D., Masse,T., Deviller,P., Kindbeiter,K., Denoroy,L. and Madjar,J.J. (1993) The herpes simplex virus type 1 US11 gene product is a phosphorylated protein found to be non-specifically associated with both ribosomal subunits. *J. Gen. Virol.*, **74**, 397–406.
3. Roller,R.J. and Roizman,B. (1992) The herpes simplex virus 1 RNA-binding protein US11 is a virion component and associates with ribosomal 60S subunits. *J. Virol.*, **66**, 3624–3632.
4. Nishiyama,Y., Kurachi,R., Daikoku,T. and Umene,K. (1993) The US 9, 10, 11, and 12 genes of herpes simplex virus type 1 are of no importance for its neurovirulence and latency in mice. *Virology*, **194**, 419–423.
5. Diefenbach,R.J., Miranda-Saksena,M., Diefenbach,E., Holland,D.J., Boadle,R.A., Armati,P.J. and Cunningham,A.L. (2002) Herpes simplex virus tegument protein US11 interacts with conventional kinesin heavy chain. *J. Virol.*, **76**, 3282–3291.
6. Mohr,I. and Gluzman,Y. (1996) A herpes virus genetic element which affects translation in the absence of the viral GADD34 function. *EMBO J.*, **15**, 4759–4766.
7. Cassady,K.A., Gross,M. and Roizman,B. (1998) The herpes simplex virus US11 protein effectively compensates for the gamma1(34.5) gene if present before activation of protein kinase R by precluding its phosphorylation and that of the alpha subunit of eukaryotic translation initiation factor 2. *J. Virol.*, **72**, 8620–8626.
8. Diaz-Latoud,C., Diaz,J.J., Fabre-Jonca,N., Kindbeiter,K., Madjar,J.J. and Arrigo,A.P. (1997) Herpes simplex virus Us11 protein enhances recovery of protein synthesis and survival in heat shock treated HeLa cells. *Cell Stress Chaperones*, **2**, 119–131.
9. Mulvey,M., Poppers,J., Sternberg,D. and Mohr,I. (2003) Regulation of eIF2alpha phosphorylation by different functions that act during discrete phases in the herpes simplex virus type 1 life cycle. *J. Virol.*, **77**, 10917–10928.
10. Attrill,H.L., Cumming,S.A., Clements,J.B. and Graham,S.V. (2002) The herpes simplex virus type 1 US11 protein binds the coterminal UL12, UL13, and UL14 RNAs and regulates UL13 expression *in vivo*. *J. Virol.*, **76**, 8090–8100.
11. Roller,R.J., Monk,L.L., Stuart,D. and Roizman,B. (1996) Structure and function in the herpes simplex virus 1 RNA-binding protein U(s)11: mapping of the domain required for ribosomal and nucleolar association and RNA binding *in vitro*. *J. Virol.*, **70**, 2842–2851.
12. Poppers,J., Mulvey,M., Perez,C., Khoo,D. and Mohr,I. (2003) Identification of a lytic-cycle Epstein–Barr virus gene product that can regulate PKR activation. *J. Virol.*, **77**, 228–236.
13. Diaz,J.J., Dodon,M.D., Schaerer-Uthurralt,N., Simonin,D., Kindbeiter,K., Gazzolo,L. and Madjar,J.J. (1996) Post-transcriptional transactivation of human retroviral envelope glycoprotein expression by herpes simplex virus Us11 protein. *Nature*, **379**, 273–277.
14. Roller,R.J. and Roizman,B. (1990) The herpes simplex virus Us11 open reading frame encodes a sequence-specific RNA-binding protein. *J. Virol.*, **64**, 3463–3470.
15. Roller,R.J. and Roizman,B. (1991) Herpes simplex virus 1 RNA-binding protein US11 negatively regulates the accumulation of a truncated viral mRNA. *J. Virol.*, **65**, 5873–5879.
16. Schaerer-Uthurralt,N., Erard,M., Kindbeiter,K., Madjar,J.J. and Diaz,J.J. (1998) Distinct domains in herpes simplex virus type 1 US11 protein

mediate post-transcriptional transactivation of human T-lymphotropic virus type I envelope glycoprotein gene expression and specific binding to the Rex responsive element. *J. Gen. Virol.*, **79**, 1593–1602.

17. Khoo,D., Perez,C. and Mohr,I. (2002) Characterization of RNA determinants recognized by the arginine- and proline-rich region of Us11, a herpes simplex virus type 1-encoded double-stranded RNA binding protein that prevents PKR activation. *J. Virol.*, **76**, 11971–11981.

18. Zuccola,H.J., Filman,D.J., Coen,D.M. and Hogle,J.M. (2000) The crystal structure of an unusual processivity factor, herpes simplex virus UL42, bound to the C terminus of its cognate polymerase. *Mol. Cell*, **5**, 267–278.

19. Cox,J.C. and Ellington,A.D. (2001) Automated selection of anti-protein aptamers. *Bioorg. Med. Chem.*, **9**, 2525–2531.

20. Cox,J.C., Rajendran,M., Riedel,T., Davidson,E.A., Sooter,L.J., Bayer,T.S., Schmitz-Brown,M. and Ellington,A.D. (2002) Automated acquisition of aptamer sequences. *Comb. Chem. High Throughput Screen.*, **5**, 289–299.

21. Bell,S.D., Denu,J.M., Dixon,J.E. and Ellington,A.D. (1998) RNA molecules that bind to and inhibit the active site of a tyrosine phosphatase. *J. Biol. Chem.*, **273**, 14309–14314.

22. Kramer,M.F. and Coen,D.M. (1995) Quantification of transcripts from the ICP4 and thymidine kinase genes in mouse ganglia latently infected with herpes simplex virus. *J. Virol.*, **69**, 1389–1399.

23. Smith,C.W.J. (1998) *RNA–Protein Interactions: A Practical Approach*. Oxford University Press, Oxford, NY.

24. Coligan,J.E. (1996) *Current Protocols In Protein Science*. Wiley, Brooklyn, NY.

25. Weisshart,K., Chow,C.S. and Coen,D.M. (1999) Herpes simplex virus processivity factor UL42 imparts increased DNA-binding specificity to the viral DNA polymerase and decreased dissociation from primer–template without reducing the elongation rate. *J. Virol.*, **73**, 55–66.